ELSEVIER

Journal of Atmospheric and Solar-Terrestrial Physics 69 (2007) 2338–2354

Journal of ATMOSPHERIC AND SOLAR-TERRESTRIAL PHYSICS

www.elsevier.com/locate/jastp

Large-scale thermodynamics of the stratosphere and mesosphere during the major stratospheric warming in 2003/2004

P. Mukhtarov[a], D. Pancheva[b,*], B. Andonov[a], N.J. Mitchell[b], E. Merzlyakov[c], W. Singer[d], W. Hocking[e], C. Meek[f], A. Manson[f], Y. Murayama[g]

[a]*Geophysical Institute, Bulgarian Academy of Sciences, Sofia, Bulgaria*
[b]*Department of Electronic and Electrical Engineering, University of Bath, Bath, UK*
[c]*Institute of Experimental Meteorology, Obninsk, Russia*
[d]*Leibniz-Institute of Atmospheric Physics, Kühlungsborn, Germany*
[e]*University of Western Ontario, London, Canada*
[f]*ISAS, University of Saskatchewan, Saskatoon, Canada*
[g]*National Institute of Information and Communications Technology, Tokyo, Japan*

Received 14 January 2007; received in revised form 18 July 2007; accepted 30 July 2007
Available online 6 August 2007

Abstract

The stratosphere–mesosphere response to the major sudden stratospheric warming (SSW) in the winter of 2003/2004 has been studied. The UKMO (UK Meteorological Office) data set was used to examine the features of the large-scale thermodynamic anomalies present in the stratosphere of the Northern Hemisphere. The vertical and latitudinal structure of the genuine anomalies, emphasized by removing the UKMO climatology, has been investigated as well. The features of the stratospheric anomalies have been related to the mesospheric ones in measured neutral winds from radars and temperatures from meteor radars (~90 km). It was found that the stratospheric warming spread to the lower mesosphere, while cooling occurred in the upper mesosphere, a feature that may be related to the large vertical scales of the stationary planetary waves (SPWs). It was shown also that the beginning of the eastward wind deceleration in the stratosphere–mesosphere system coincided with the maximum amplification of the SPW1 accompanied by short-lived bursts of waves 2 and 3.

Keywords: Sudden stratospheric warming; Polar vortex; Stationary planetary waves; Wave–mean flow interaction

1. Introduction

The sudden stratospheric warming (SSW) is a transient large-scale thermodynamical phenomenon which occurs and strongly affects the winter middle atmosphere, causing significant variations in the MLT region as well. It involves considerable changes of the background wind, temperature, planetary and gravity wave activity and redistributes ozone and other chemicals in high latitudes. This event was discovered by Scherhag (1952, 1960). It is known that before the onset of the SSW, the stratospheric circulation is dominated by a cold and strong eastward polar vortex (a region of high atmospheric vorticity, beginning just above the tropopause and reaching maximum wind speed

*Corresponding author. Tel.: +44 1225 386310; fax: +44 1225 386305.
E-mail address: eesdvp@bath.ac.uk (D. Pancheva).

1364-6826/$ - see front matter © 2007 Elsevier Ltd. All rights reserved.
doi:10.1016/j.jastp.2007.07.012

near the stratopause), which lies over the North Pole, covering most of the Northern Hemisphere (NH) outside the tropics. During a major SSW, the polar vortex is almost entirely broken down and the mean fields undergo dramatic changes. The mean eastward winds are replaced by westward winds and the warm air in the stratosphere takes the place of cold air at high latitudes (Schoeberl, 1978).

The key mechanism behind the SSW, initially proposed by Matsuno (1971) and now widely accepted, relates to the growth of upward propagating transient planetary waves and their non-linear interaction with the zonal mean flow. The interaction decelerates and/or reverses the eastward winter winds and also induces a downward circulation in the stratosphere causing adiabatic heating and an upward circulation in the mesosphere causing adiabatic cooling (Liu and Roble, 2002, 2005).

While the stratospheric manifestations of SSWs are reasonably well characterized from observational (Labitzke, 1965; Randel and Boville, 1987; Labitzke and Naujokat, 2000; Perlwitz and Graf, 2001) and modelling points of view (Schoeberl, 1978; Lordi et al., 1980; Hartman, 1983; Mechoso et al., 1985), the MLT manifestations are less experimentally documented and not so well understood. The initial MLT response seen in the neutral winds has been reported by Gregory and Manson (1975) and Lysenko et al. (1975), while that in the temperature by Labitzke (1972) and Myrabø et al. (1984). Later, the investigations of case studies have shown that a weakening and/or reversal of the dominating eastward directed zonal winds is seen in the MLT region as well and that the planetary wave activity is usually amplified before and during the SSW events (Cevolani, 1989; Manson and Meek, 1991; Singer et al., 1992; Hoffmann et al., 2002; Jacobi et al., 2003; Dowdy et al., 2004). The observational papers reporting the MLT response of the temperature revealed that the stratospheric warmings are usually accompanied by mesospheric coolings (Whiteway and Carswell, 1994; Walterscheid et al., 2000; Cho et al., 2004). In addition, recent studies found that the mesospheric cooling and deceleration or reversal of the mesospheric zonal wind at high winter latitudes were observed several days before the onset of the SSW in the stratosphere (Walterscheid et al., 2000; Dowdy et al., 2004).

The Sounding of the Atmosphere using Broadband Emission Radiometry (SABER) instrument on the TIMED (Thermosphere, Ionosphere, Mesosphere, Energetics and Dynamics) satellite measures global temperature at high vertical resolution from the lower stratosphere to the lower thermosphere. Siskind et al. (2005) used SABER data to quantify the relationship between temperatures in the stratosphere and in the mesosphere and lower thermosphere during three disturbed winter periods: February 2002 (major SSW) and February 2003 (minor SSW) in the NH and August 2002 (minor SSW) in the Southern Hemisphere (SH). The authors found a clear signature of mesospheric cooling in concert with stratospheric warming. Their analysis indicated a significant anticorrelation only between the temperature at 10 hPa and mesospheric temperatures for pressure levels between 0.7 and 0.01 hPa. For altitudes higher than 80 km (pressures <0.01 hPa) no correlation with the stratospheric temperature was seen. Based on this result, the authors suggested that the vertical depth of the mesospheric cooling associated with the stratospheric warming seems to be smaller than that predicted with the TIME-GCM (Liu and Roble, 2002), but it agrees well with the general morphology shown by the hindcasting simulation of the August 2002 minor SSW observed in the SH made by Coy et al. (2005).

The present work is focused on the large-scale temperature and zonal wind anomalies observed in the stratosphere and mesosphere during the Arctic winter of 2003/2004 and the period of time between 1 October 2003 and 30 April 2004 is investigated thoroughly. A major SSW took place in December/January, which was particularly remarkable because it consisted of a period of nearly 2 months of polar vortex disruption and a reversed direction of the zonal mean flow observed in the middle and lower stratosphere (Manney et al., 2005). The UK Meteorological Office (UKMO) temperature and zonal wind data have been used to explore the vertical and latitudinal structure of the large-scale anomalies in thermodynamics of the NH stratosphere. The mesospheric anomalies related to the major SSW in 2003/2004 have been identified in the radar measurements of neutral winds and temperature (around 90 km height).

2. Observations and data analysis

2.1. UK Meteorological Office data

The UKMO data set is used to examine the features of the large-scale thermodynamic disturbances present in the winter of 2003/2004 stratosphere of the NH.

This data set is a result of assimilation of in situ and remotely sensed data into a numerical forecast model of the stratosphere and troposphere. The description of the original data assimilation system can be found in Swinbank and O'Neill (1994), while the new three-dimensional variational system can be found in Swinbank and Ortland (2003). The outputs of the assimilation are global fields of daily temperature, geopotential heights and wind components at pressure levels from the surface up to 0.1 hPa. The generated data fields have global coverage with 2.5° and 3.75° steps in latitude and longitude, respectively. The UKMO data well represent the global features of stratospheric thermodynamics and have been used by many researchers to study different dynamical events in the stratosphere including planetary waves (Fedulina et al., 2004) and SSWs (Dowdy et al., 2004; Cho et al., 2004).

The UKMO temperature and zonal wind data at four pressure levels (30, 10, 1 and 0.3 hPa) are used to explore the features of the large-scale thermodynamic processes in the NH stratosphere. It was mentioned before that the key mechanism behind the SSW is related to the growth of the transient planetary waves present in the winter stratosphere. The most important are stationary Rossby planetary waves (SPWs), which propagate upward from the troposphere and are very strong but quite variable during winter. Travelling planetary waves are also present in the UKMO data. To determine the predominant periods of the planetary waves, we use spectral analysis which is a two-dimensional analogue of the Lomb–Scargle periodogram method based on the least-squares fitting procedure applied to the entire time series. The planetary waves with periods between 5 and 30 days and with zonal wavenumbers up to 3 are studied. The main purpose is not only to define the predominant periods of the wave components which contribute to the variability of the atmospheric fields but also to isolate and study them in detail. To extract the waves from the data or to determine their amplitudes and phases, we use again a least-squares fitting procedure, but this time it is applied to the time segment twice the length of the longest period under investigation. Then this segment is moved through the time series with steps of 1 day in order to obtain the daily values of the wave amplitudes and phases. The planetary wave structures (SPWs and travelling planetary waves together) are viewed in the geopotential height data (the height of a given pressure level) for the above-mentioned four pressure levels. Only the features of the SPWs (with frequency equal zero) will be examined in this study to indicate their effect on the course of the major SSW. The planetary wave coupling of the stratosphere and mesosphere during this SSW event will be investigated in a separate study.

2.2. MLT measurements

We use zonal wind data from eight radars situated at middle and high latitudes and predominantly in the western part of the NH (Table 1). Three of these radars are commercially produced: SKiYMET all-sky VHF systems located at Esrange (68°N, 21°E), Andenes (69°N, 16°E) and Yellowknife (63°N, 114°W). The radar at Esrange uses a solid-state transmitter of 6 kW peak power and transmits at a frequency of 32.5 MHz with a pulse repetition frequency of 2144 Hz. The Andenes meteor radar operates with the same parameters except for the higher peak power of 12 kW. The radar at Yellowknife is a standard SKiYMET system and some details for it can be found in Hocking et al. (2001). The all-sky meteor radar used in this study applies crossed antenna elements on

Table 1
Geographic locations of the radars, the type of the instrument and the height range of available measurements

Station	Instrument	Location	Height range (km)
Andenes	SKiYMET	69°N, 16°E	82–98
Esrange	SKiYMET	68°N, 21°E	81–97
Poker Flat	MF radar	65°N, 147°W	50–108 (only data for the range of 60–90 km are used)
Yellowknife	SKiYMET	63°N, 114°W	82–98
Obninsk	Meteor radar	55°N, 37°E	No height resolution
Kuehlungsborn	MST (meteor mode)	54°N, 12°E	85–94
Castle Eaton	Meteor radar	53.5°N, 3.9°W	No height resolution
Saskatoon	MF radar	52°N, 107°W	67–94

transmission and reception to ensure a near-uniform azimuthal sensitivity to meteor echoes. The system uses a five-antenna interferometer on reception, resulting in a range accuracy of 2 km and an angular accuracy of about 2° in meteor location. The meteor echo azimuth and zenith angles combined with the range information provide the height of the meteor echo. A detailed description of the data handling and the process used to produce wind velocities from individual meteor echoes can be found in Hocking et al. (2001). Routine data analysis yields hourly spaced values of the zonal and meridional winds at six independent height intervals between 81 and 97 km height for Esrange radar (for more details see Mitchell et al., 2002) and between 82 and 98 km height for the radars at Andenes and Yellowknife (Singer et al., 2003; Hocking et al., 2001).

The radars at Obninsk (55°N, 37°E) and Castle Eaton (53.5°N, 3.9°W) are meteor radars (beam system) without height information. Their measurements represent a sampling of the winds in the MLT region with weighting reflecting the vertical distribution of meteor echoes. This distribution is strongly peaked at heights near 90 km. The radar at Kuehlungsborn (54°N, 12°E) is an MST radar working in meteor mode during the investigated period of time.

Two of the radars are medium-frequency radars (MFR) and are located at Saskatoon (52°N, 107°W) and Poker Flat (65°N, 147°W). The two radars are of similar configuration and their detailed descriptions can be found in Manson et al. (1973) and Murayama et al. (2000). MFRs employ the spaced antenna technique to detect motions of weakly ionized irregularities in the ionospheric D and lower E regions. The basic analysis applied to the complex radar signals at Saskatoon and Poker Flat is the full correlation analysis (FCA). The radars provide samples of wind every 2 or 3 km and 2 or 5 min on a continuous basis and these data were used to obtain the hourly mean winds. Usually, the coverage is poorest at low heights due to the increased noise level and lack of useful radar scatter during the night below ~70 km, but it becomes better near and above 80 km. Only zonal wind data up to 90 km height are used for Poker Flat radar and up to 94 km for Saskatoon radar.

The basic information used in this study consists of daily estimates of the prevailing zonal wind at each of the height intervals. Daily zonal winds are found from radar hourly data by least-squares fit of mean, 24-, 12- and 8-h components to each day's data provided there are 16 or more hourly values available.

The temperature anomalies in the MLT region are studied by the SKiYMET radars. This radar method for estimating the daily temperature data at the height of maximum meteor detectability (which depends on frequency, season and location and it is in the range of 86–92 km, we will label it 90 km) is based on the meteor decay times (for details see Hocking, 1999; Hocking et al., 2004). The typical accuracy of these measurements is on average ~5–7 K. The method is more accurate in the non-summer months, when the temperature gradient can be better and more reliably represented.

3. Large-scale anomalies in the stratosphere

3.1. Vertical structure of anomalies at 60°N

The major SSW is defined as an event where both the zonal mean temperature gradient and zonal mean zonal winds at 10 hPa pressure level reverse sign poleward of 60°, and is why we study the vertical structure of the temperature and zonal wind anomalies in detail there.

The upper plot of Fig. 1 shows the altitude–time cross section of the UKMO zonal mean temperature, while the bottom plot shows the zonal mean zonal wind at 60°N. The altitude range between 20 and ~60 km height is investigated. Fig. 1 shows that during normal winter conditions, the stratosphere is dominated by a cold and strong eastward zonal mean zonal wind. The stratopause, around 55 km height, is clearly outlined in the temperature plot (upper). A large temperature anomaly with reversed temperature gradient can be distinguished between days 60 (end of November 2003) and 100 (beginning of January 2004). This anomaly is composed of three pulses. The first of them occurs around day 70 and reaches only 40 km height. This disturbance is accompanied by rapid deceleration of the zonal mean zonal wind (bottom plot). The second pulse is centred around day 85 and it is the strongest pulse (with the largest temperature gradient) within the temperature anomaly observed between days 60 and 100. The effects are seen down to 26–27 km height. The deceleration of the zonal mean circulation (bottom plot) continues rapidly and it reverses to westward (breakdown of the polar vortex) around day 80. The reversal of the zonal mean zonal wind,

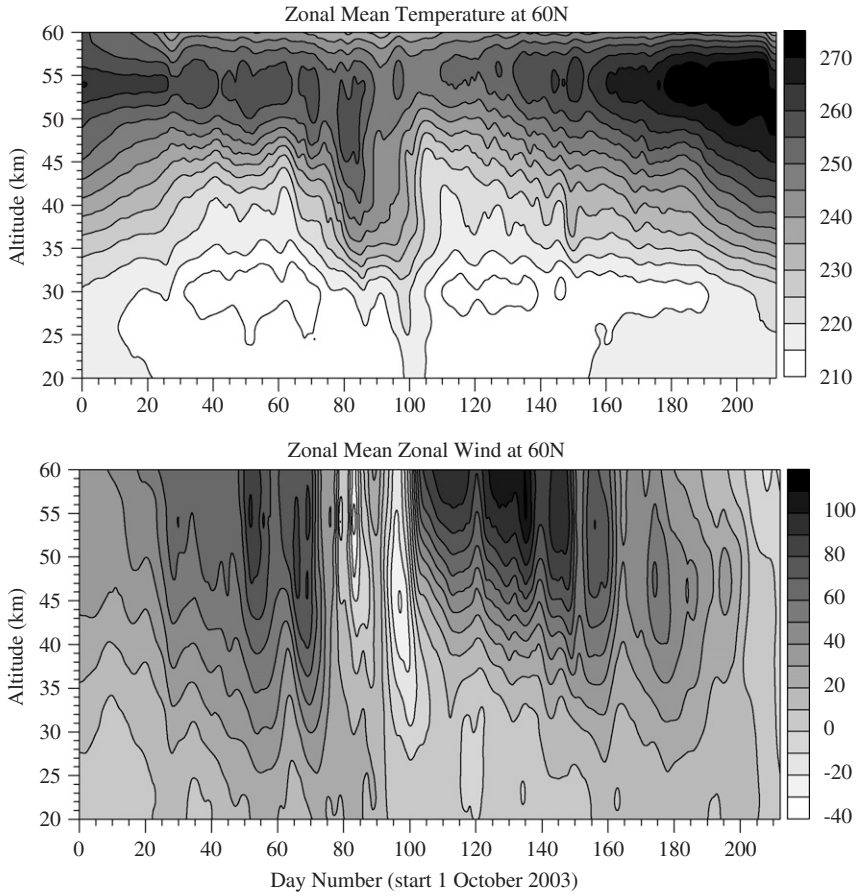

Fig. 1. Altitude–time cross section of the UKMO zonal mean temperature (upper plot) and zonal mean zonal wind at 60°N (bottom plot).

however, does not extend lower than 40 km height. The mean circulation at 10 hPa pressure level (~32 km height) continues to be westward at that time, i.e. the condition for a major SSW has not yet been fulfilled. The third temperature pulse (upper plot) develops around days 90–100 and it is accompanied by a new reversal of the mean zonal flow and this time the reversal extends to ~25 km height. The zonal mean zonal wind becomes westward at 10 hPa and at 60°N around day 95 and this defines the onset of the major SSW. After around day 100 the stratosphere rapidly becomes cold and the westward mean circulation is replaced by a normal winter eastward circulation. This, however, is observed mainly in the upper stratosphere (above 10 hPa) where the circulation is strengthened significantly till around day 160 (middle of March). In the middle and lower stratosphere, a new reversal of the mean circulation occurs around day 120 and the disruption of the polar vortex reaches the lowest heights during this winter.

Fig. 1 reveals the complex character of the major SSW event during the winter 2003/2004, which is composed of three temperature and zonal mean zonal disturbances clearly delineated at 60°N. Each subsequent warming event affects a greater part of the stratosphere. Quiroz (1971) suggested that they start in the upper stratosphere and move down to the lower levels. Fig. 1 also reveals that the downward penetration of the disturbances in the stratosphere occurs with some delay with respect to the upper levels and this effect is particularly visible in the zonal mean zonal wind (bottom plot). To define this delay, the cross-correlation function between the zonal mean zonal wind at the 0.1 hPa pressure level (~59 km height) and all lower levels was calculated and only data for the disturbed period of time (between days 60 and 120) were used. Fig. 2 shows the cross-correlation function in the

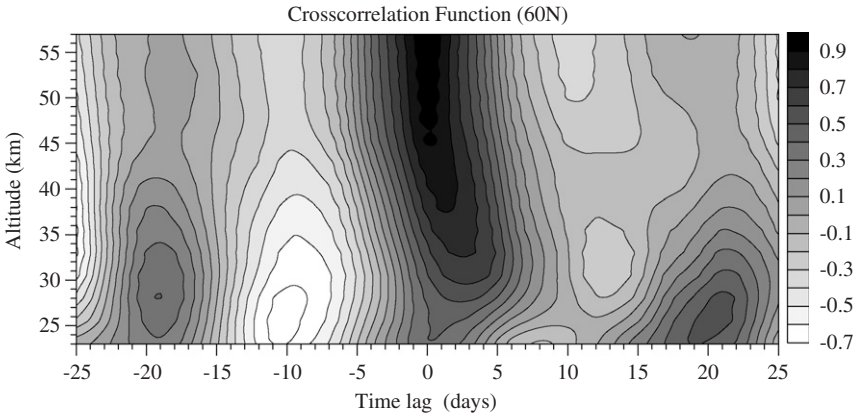

Fig. 2. Cross-correlation function in the altitude range of 23–52 km calculated between the UKMO zonal mean zonal wind at the 0.3 hPa pressure level and all lower levels; only data for the disturbed period of time (between days 60 and 120) were used.

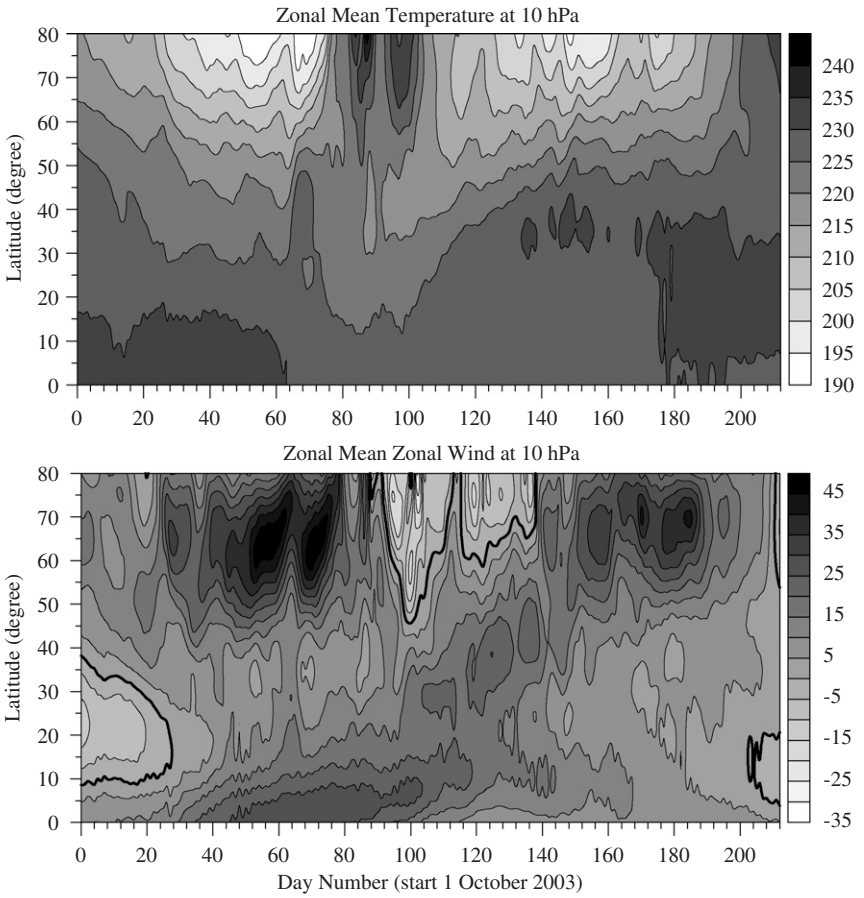

Fig. 3. Latitudinal structure of the UKMO zonal mean temperature (upper plot) and zonal mean zonal wind (bottom plot) anomalies at the 10 hPa pressure level; a thick solid line represents the wind zero-line.

altitude range between 23 and 52 km with time lags up to 25 days. It is characterized by two features: (i) the central maximum clearly indicates the delay of the wind reversal with decreasing altitude; this delay is noticeable below 45 km height and it reaches 3 days at an altitude of 30 km and (ii) the secondary

maxima situated at a time lag of about ± 20 days reflect the presence of the planetary wave disturbances visible in the UKMO zonal mean zonal wind (bottom plot of Fig. 1). The oscillations observed in the zonal mean zonal wind should not depend on the longitude and such a type of wave is known to be a zonally symmetric wave. Figs. 1 and 2 indicate that stratospheric dynamics during the winter of 2003/2004 is strongly dominated by the presence of zonally symmetric waves. These have been studied in detail by Pancheva et al. (2007).

3.2. Latitudinal structure of anomalies at 10 hPa

Fig. 3 shows the latitudinal structure of the zonal mean temperature (upper plot) and zonal mean zonal wind (bottom plot) anomalies at a 10 hPa pressure level. The SSW event at ~32 km height is composed of two warming pulses. They occur around days 85 and 95 and are observed at latitudes higher than 50°N. These two warming pulses at high latitudes are associated with cooling observed at low–middle and tropical latitudes (30–40°N). After around day 105 the temperature rapidly decreases at high latitudes.

Both warming pulses are related to reversals of the zonal mean flow (the thick solid line represents the wind zero-line); however, the first reversal is limited only to very high latitudes, while the second one reaches 45°N and is present till day 110. An interesting event is observed after day 110: although the temperature at high latitudes decreases rapidly after day 105, a new reversal of the zonal mean flow occurs until day 140 (middle of February 2004). Altogether, the polar vortex at 10 hPa and at latitudes higher than 60°N was disrupted for more than $1\frac{1}{2}$ months. Similarly to the temperature, the high-latitude reversed zonal flow is associated with strengthened eastward flow observed at low–middle and tropical latitudes.

3.3. Vertical and latitudinal structure of anomalies with removed UKMO climatology

The large-scale thermodynamic processes being studied here in relation to the major SSW in 2003/2004 include regular seasonal variability of the zonal mean temperature and zonal mean zonal wind. Therefore, to find the genuine anomalies characterizing this particular SSW we have to remove the UKMO climatology. The monthly mean data for the temperature and zonal wind between 1992 and 2005 (or 14 years) were used for calculating the UKMO climatology. The daily time series were obtained by approximating the mean seasonal variation with trigonometric polynomials. We consider four pressure levels: 30, 10, 1 and 0.3 hPa in order to study the vertical structure of the genuine anomalies in the latitudinal range between the equator and 80°N.

Fig. 4 shows the latitude–time cross sections of the differential temperature at the four above-mentioned pressure levels. We use the same scale in order to compare the anomalies at different levels. We note that the temperature variations related to the major SSW at the upper most level are weak, but this level is very close to the stratopause where the height gradients are small. In general, the overall vertical and latitudinal structure of the genuine temperature anomalies is very similar to that discussed in the previous two sections. That is (i) the positive temperature excursions associated with the major stratwarm are related to increasing delay with lower height and (ii) the positive temperature excursions at high latitudes are associated with negative ones at low–middle and tropical latitudes; this latter "compensating" effect is particularly strong at 1 hPa (~48 km height) where the negative temperature pulses amplify towards the equator. Fig. 4 shows also that whereas the positive anomaly related to the SSW at 30 hPa continues till day 140, the negative anomaly at 1 hPa intensifies significantly during this time.

Fig. 5 shows the latitude–time cross sections of the zonal mean zonal wind minus the climatology at the same pressure levels with a fixed scale. As with temperature, the main features of the genuine wind anomalies are similar to those discussed before the UKMO climatology was removed, but there are also some peculiarities that should be noticed. While the negative wind excursions at 1 and 0.3 hPa occur almost simultaneously a clear delay is observed for those at 10 and 30 hPa in accordance with the cross-correlation function result shown in Fig. 2. As we have already mentioned, the dynamical regime of the upper stratosphere/lower mesosphere (1 and 0.3 hPa) appears to be different from that in the middle and lower stratosphere (10 and 30 hPa) after the onset of the major SSW. The significant strengthening of the polar vortex in the upper stratosphere and its disruption in the middle and lower stratosphere can be clearly distinguished in the figure. It is worth mentioning, however, that the strengthening of the polar vortex immediately after

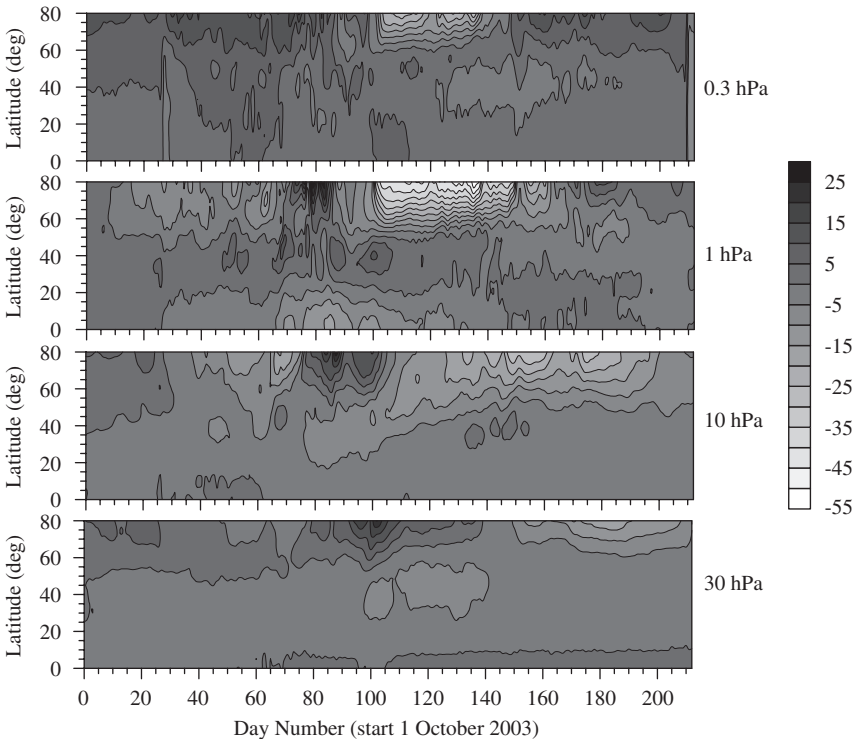

Fig. 4. Latitudinal structure of differential temperature (UKMO climatology was removed) at four pressure levels: 30, 10, 1 and 0.3 hPa. The same scale is used for all height levels to facilitate the comparison at different levels.

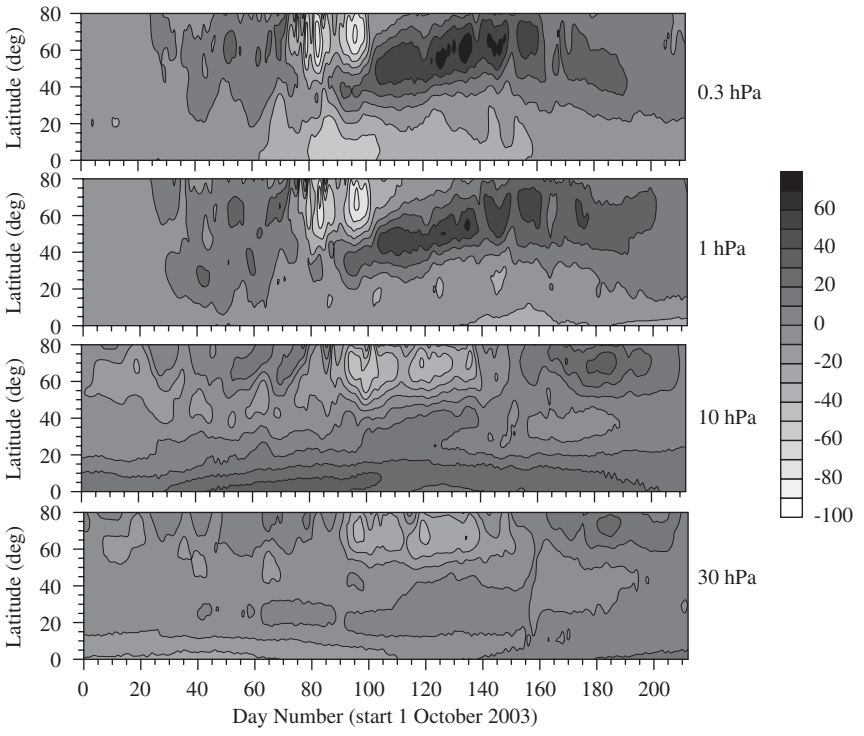

Fig. 5. The same as Fig. 4, but for the zonal mean zonal wind.

the onset of the major SSW in the upper stratosphere starts at latitudes around 50–60°N and moves northward reaching latitudes of 70–75°N near day 140. The negative wind anomalies at high latitudes are linked with the positive anomalies at low–middle and tropical latitudes and this effect is particularly strong in the upper stratosphere. Another interesting effect is visible at 0.3 hPa: there is a connection between the negative wind anomalies at high latitudes and alternating regions of positive anomalies in low–middle and tropical latitudes and again a negative anomaly in the equatorial latitudes. This effect clearly demonstrates a strong latitudinal coupling of the thermodynamic processes in the upper stratosphere/lower mesosphere during the major stratwarm in the winter of 2003/2004. It is also worth noting that in the period 1992–2005 the strongest UKMO westward zonal mean zonal wind at a 0.3 hPa pressure level over the equator occurs during the winter of 2003/2004.

4. Stratosphere–mesosphere anomalies related to the major SSW

We study the mesosphere thermodynamic response to the major SSW in the winter of 2003/2004 by using eight radars. Table 1 lists the radar locations, the type of the instrument and the height range of available measurements. It is particularly noted that only wind measurements in the height range of 60–90 km have been used for Poker Flat because of many gaps above 90 km. An advantage of the MF radars with respect to the SKiYMET radars is that they offer wind measurements at lower heights, while the SKiYMET radars offer wind measurements the at upper mesosphere and lower thermosphere (80–100 km height). We use this advantage to explore first the large-scale zonal wind anomalies linked to the major SSW in the stratosphere–mesosphere above Poker Flat and Saskatoon. Fig. 6 shows the altitude–time cross sections of the zonal winds modelled and measured at Poker Flat (upper plot) and at Saskatoon (middle plot) during the winter of 2003/2004. The height range from 23 km (~30 hPa) to 90 km for Poker Flat and to 94 km for Saskatoon is shown in the plots. The stratospheric UKMO zonal wind data are for the geographical locations of Poker Flat and Saskatoon, respectively, and cover the pressure levels between ~30 and ~0.3 hPa. Both plots show almost simultaneous zonal wind reversals during the SSW event and in this way the interrelation of the reversal pulses in the stratosphere and mesosphere is clearly outlined. It is also evident that the strongest westward winds are observed around 45–55 km height. There is a clear association between the planetary wave disturbances observed in the stratosphere and mesosphere and this relationship is particularly well outlined at Saskatoon. Some differences between the winds at both locations can be distinguished as well. They are visible in (i) the amplitudes of the zonal wind variability, (ii) the strength of the jet before and after the onset of the SSW and (iii) the timing of the pulses. These differences might be attributed predominantly to the latitudinal than to the longitudinal differences of both stations.

We use again the cross-correlation analysis in order to find a quantitative relationship between the zonal wind large-scale anomalies in the stratosphere–mesosphere system. Only Saskatoon wind data have been used for this purpose, because the number of gaps is smaller than those at Poker Flat. The cross-correlation function between the zonal wind at 0.3 hPa pressure level and all lower and upper levels was calculated and only data for the disturbed period of time (between days 60 and 120) were used. The bottom plot of Fig. 6 shows the cross-correlation function calculated in the height range between 23 and 94 km with a time lag up to 25 days. It is characterized by two features: (i) the central maximum clearly indicates that there is almost no delay of the wind reversals between 56 km height and all upper levels in the mesosphere and as in Fig. 2, there is some delay with decreasing altitude in the stratosphere, which is clearly seen below 40–45 km height and it reaches 5 days at an altitude of 30 km and (ii) there are secondary maxima situated at a time lag of about $\pm$20–25 days, which reflect the presence of long-period planetary wave disturbances present in the stratosphere–mesosphere system over this location. Planetary wave coupling of the stratosphere–mesosphere system will be discussed in a separate study.

Eastward zonal winds normally dominate the winter mesosphere, at least up to 90–95 km height. However, there are two periods of westward zonal winds that occurred in the high-latitude station Poker Flat before the two main reversal pulses (see the upper plot of Fig. 6) related to the SSW. A comparison of the mesospheric mean zonal wind measured at 80 km height with the zonal mean zonal wind derived from the UKMO stratospheric data at

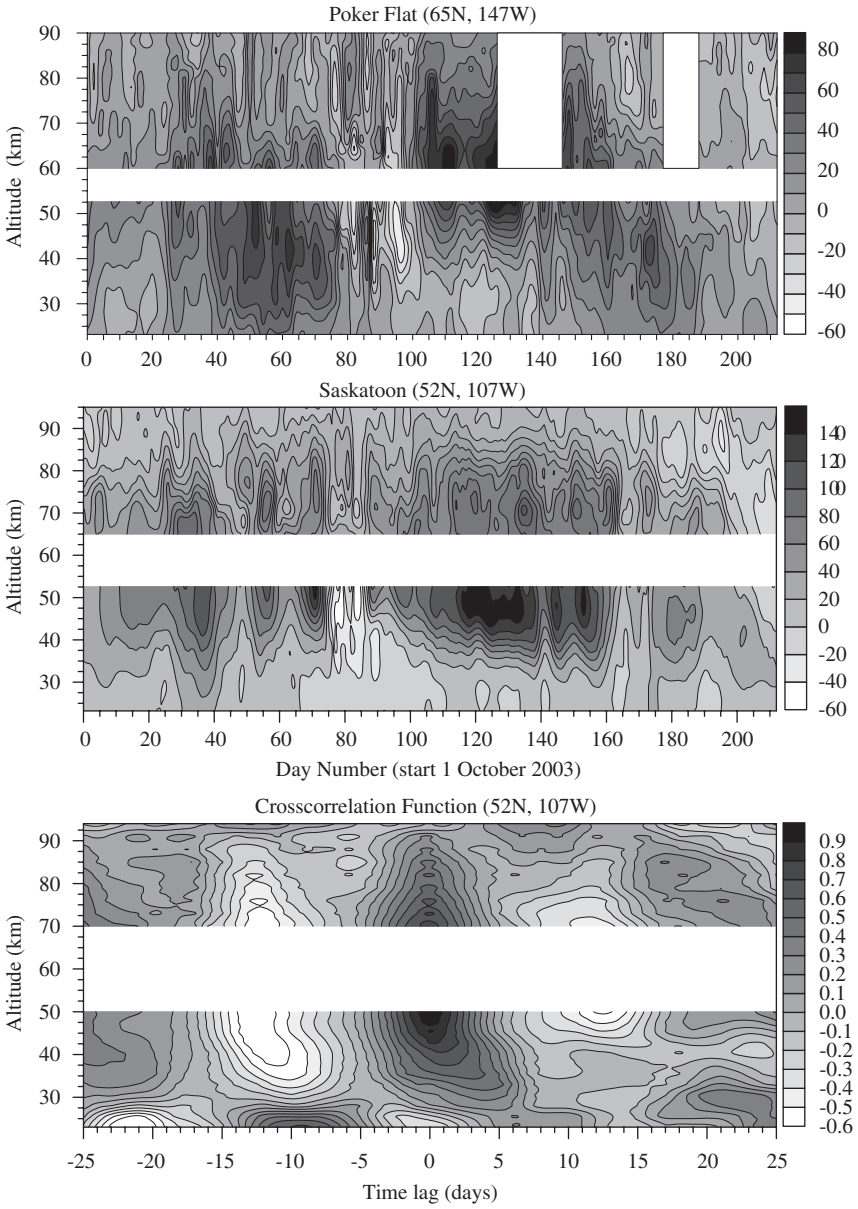

Fig. 6. Altitude–time cross sections of the zonal winds measured at Poker Flat (upper plot) and at Saskatoon (middle plot) during the winter of 2003/2004. The stratospheric zonal wind data are for the geographical locations of Poker Flat and Saskatoon, respectively, and cover the pressure levels between 30 and 0.3 hPa. The bottom plot shows the cross-correlation function calculated only for Saskatoon between the zonal wind at the 0.3 hPa pressure level and all lower and upper levels; only data for the disturbed period of time (between days 60 and 120) were used.

10 hPa during the major SSW in the SH in the winter of 2002 made by Dowdy et al. (2004) showed that the reversal event in the mesosphere preceded that in the stratosphere by several days (~6–7 days). A similar analysis is done in this study in order to find out how the reversal of the mean zonal wind in the mesosphere varies with altitude and latitude, as well as to compare it with that found by Dowdy et al. (2004).

First, the zonal wind at high latitudes will be studied. We have only four radars situated at latitudes higher than 60°N covering half of the parallel circle and cannot obtain the exact zonal mean zonal wind, so their average at a height of

81–82 km will be used as a an approximation of the zonal mean zonal wind in the latitude range 63–69°N. Fig. 7 shows the comparison between the mean zonal wind at ~80 km in the high latitudes (middle plot; the error bars indicate the standard deviation of the mean) and the UKMO zonal mean zonal wind at 10, 1 and 0.3 hPa pressure levels averaged for the latitude range of 60–70°N (upper plot). The onset of the major SSW is at day 94 (2 January 2004) and it is defined by the zonal mean zonal wind reversal at 10 hPa. The reversals of the zonal mean zonal winds at 1 and 0.3 hPa occur simultaneously almost 2 weeks before the onset of the SSW (first short reversal is on day 79 followed by one on day 82). The variability of the mean zonal wind in the high-latitude MLT region around the onset of the SSW shows the same two-peak structure as that of the zonal mean zonal wind in the upper stratosphere and the reversal of the wind at ~80 km height is on day 85. This reversal is 9 days before the onset of the SSW, but slightly after the reversal of the zonal mean zonal wind at 1 or 0.3 hPa. We have to keep in mind that the stratospheric zonal mean zonal wind is averaged for the latitudinal range of 60–70°N, while the radars are situated between 63° and 69°N and that the MLT mean zonal wind at ~80 km is an approximation of the zonal mean zonal wind at this altitude; therefore, in general, the above-obtained comparisons indicate that the upper stratosphere and mesosphere (~80 km height) mean zonal wind reversal happens almost simultaneously about 10–14 days before the onset of the SSW. The mean zonal wind reversal in the MLT region, however, is very weak and the westward wind is only 5–6 m/s.

To find out how the reversal of the mean zonal wind in the mesosphere depends on the altitude, we calculate the mean zonal wind measured by the same radars located in the latitudes higher than 60°N, but for the heights 90–91 km. The result is shown by a thin solid line in the bottom plot of Fig. 7. In order to facilitate the comparison, the mean zonal wind at ~80 km height is shown again in this plot and it is marked by a thick solid line. The reversal of the mean zonal wind at ~90 km height not only precedes that at ~80 km by 2 days (day 83), but also reaches a higher westward velocity, ~12–14 m/s.

The latitudinal dependence of the mean zonal wind reversal in the mesosphere is studied by wind measurements from four radars (Obninsk, Kuehlungsborn, Castle Eaton and Saskatoon) situated at

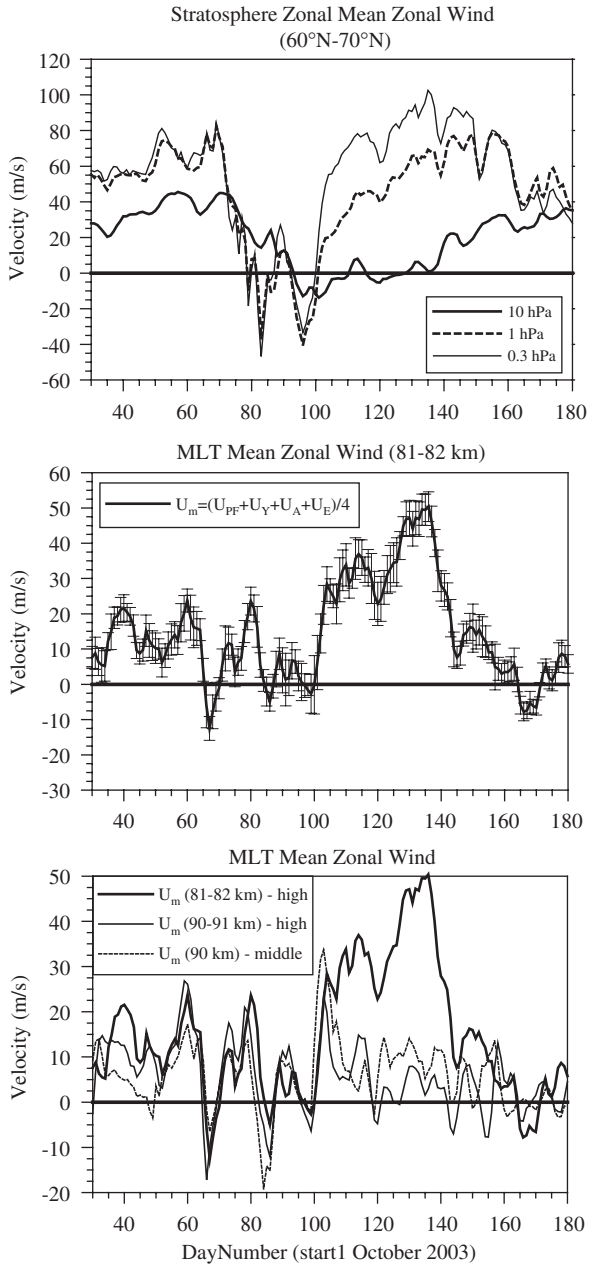

Fig. 7. Zonal mean zonal winds at 10, 1 and 0.3 hPa pressure levels averaged for a latitude range of 60–70°N is shown in the upper plot; the wind at 10 hPa is marked by a thick solid line, at 1 hPa by a thick dash line and at 0.3 hPa by a thin solid line. Mean high-latitude zonal wind at 81–82 km height obtained by averaging the zonal winds measured at Esrange, Andenes, Yellowknife and Poker Flat is presented in the middle plot; the error bars indicate the standard deviation of the mean. The bottom plot shows the mean high-latitude zonal wind at ~90 km height (think solid line) and the mean middle latitude zonal wind at ~90 km height (thin small dash line) obtained by averaging the zonal winds measured at Obninsk, Kuehlungsborn, Castle Eaton and Saskatoon; to facilitate comparison, the mean high-latitude zonal wind at ~80 km is shown again (thick solid line).

high–middle latitudes (52–55°N). In this case, we can obtain only the mean zonal wind at ~90 km height because two of the radars (Obninsk and Castle Eaton) have data only for this level. The result is shown by a small thin dash line in the bottom plot of Fig. 7. The reversal of the mean zonal wind (~90 km) at middle latitude precedes that at high latitudes only by 1 day, but it reaches the highest westward velocity, ~20 m/s.

We have already mentioned in Section 2 that the mesospheric temperature around 90 km height can be determined from radar-meteor decay time (Hocking, 1999).There are three SKiYMET radars located in the latitude range between 63° and 69°N (see Table 1) and their measurements are used to determine the mean mesosphere temperature around 90 km height. We use this mean temperature as an approximation of the zonal mean temperature at around 90 km height and for the latitudes between 63° and 69°N. The mean MLT temperature is shown in Fig. 8 (bottom plot; the error bars indicate the standard deviation of the mean). The variability of the MLT temperature is compared with the variability of the zonal mean temperature at 10, 1 and 0.3 hPa pressure levels averaged for the latitude range of 60–70°N (Fig. 8, upper plot). The three temperature pulses described before in Section 3.1 and well visible in Fig. 1 (upper plot) are most clearly outlined here at the 1 hPa pressure level. They, however, can be seen at 0.3 hPa as well, where the last pulse, responsible for the onset of the SSW, is particularly strong. The middle plot of Fig. 8 shows the latitudinal variability of the zonal mean temperature at 0.3 hPa. The results for the latitude range of 55–70°N are shown in the figure. The three temperature pulses can be seen at all latitudes. This indicates that the major SSW in winter 2003/2004 has spread out into the lower mesosphere and to the high–middle latitudes. The expansion of this SSW to the middle latitudes can also be seen in the upper plot of Fig. 3 where the temperature pulse at 10 hPa centred around day 85 reaches latitudes close to 50°N.

It is known that usually the SSW is accompanied by mesospheric cooling. In general, this feature can be seen in Fig. 8 (bottom plot). The mesospheric cooling centred near the onset of the SSW (day 94) is observed between days 85 and 105 and has an amplitude of ~25 K. It is a clear response to the last temperature pulse observed in the stratosphere and lower mesosphere (0.3 hPa pressure level). There is however a strong negative MLT perturbation

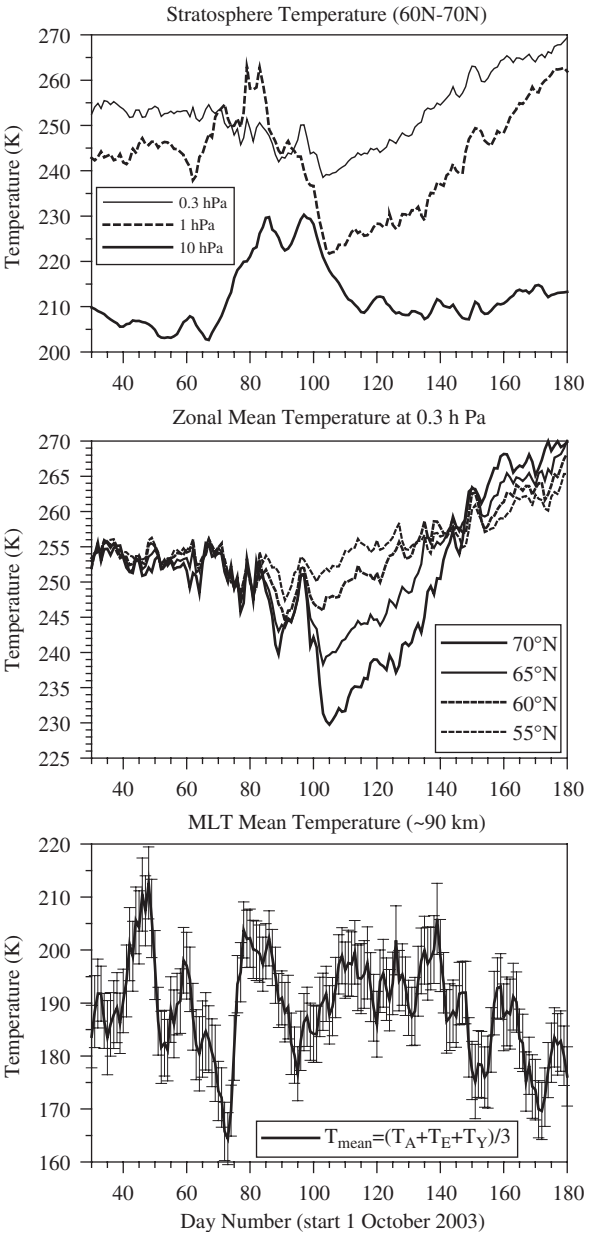

Fig. 8. Zonal mean temperature at 10, 1 and 0.3 hPa pressure levels averaged for the latitude range of 60–70°N is shown in the upper plot. The middle plot presents the latitudinal variability of the zonal mean temperature at 0.3 hPa and the results for the latitude range of 55–70°N is shown there. The mean MLT temperature around ~90 km is shown in the bottom plot; it is obtained by averaging the temperatures measured at Esrange, Andenes and Yellowknife (the error bars indicate the standard deviation of the mean).

centred around day 70, which is a response to the first temperature pulse seen in the upper stratosphere (1 hPa) and lower mesosphere (0.3 hPa). To quantify the relationship between the temperature

variability in the stratosphere and mesosphere we perform a cross-correlation analysis of the mean MLT temperature (~90 km) with the three zonal mean temperatures at 10, 1 and 0.3 hPa. Similarly to the previous cases, we include data only from the disturbed period between days 60 and 120 (December/January). Before performing the correlation analysis, all time series have been detrended in the same way—by removing a 31-day running mean (we note that the results from this type of detrending the UKMO data are almost the same as that by removing the UKMO climatology). The only statistically significant relationship at the 95% confidence level was that between the temperature at the 0.3 hPa pressure level and that at ~90 km height with the maximum correlation coefficient $R = -0.39$ (the 95% confidence interval is between -0.17 and -0.59). The correlation with the temperature at the 1 hPa level was also negative; however, the upper 95% confidence bound was close to zero, while no correlation with the 10 hPa temperature was seen.

5. Stationary planetary wave analysis

Figs. 7 and 8 also indicate that the strongest disturbances of the mean zonal wind in the MLT region causing significant deceleration of the winter jet and the strongest negative anomaly in the MLT mean temperature (~90 km) are observed near days 65–70. This period of time coincides with the beginning of the eastward wind's deceleration in the stratosphere and with the first positive temperature pulse that occurs in the upper stratosphere. Apparently, such a large-scale perturbation of the thermodynamic regime in the stratosphere and mesosphere is related to the amplification of the SPWs, which are a key agent in driving SSW events. Observations of stationary wave structure are commonly viewed using the geopotential height data. We extracted SPWs with zonal wavenumbers up to 3 from the UKMO geopotential height data. Fig. 9 shows the altitude–time cross sections of the wave amplitudes at four pressure levels: 30, 10, 1 and 0.3 hPa. The strongest, SPW1 (left column of plots), reaches amplitudes up to 1600 gpm and its first maximum is observed between days 60 and 70. This first amplification apparently plays the basic role in generating the major SSW. The SPW1 component contributes to the bulk of westward forcing before the SSW (Liu and Roble, 2002). Most probably this is the reason the stratosphere–mesosphere winter jet is so weak after days 65–70. The middle column of plots shows the amplitude of SPW2; this wave is amplified around the maximum of the SSW and reaches amplitudes up to 400 gpm. The amplitude of SPW3, shown on the right column, is also large around the maximum of the SSW but its amplitude is significantly weaker, up to 105 gpm. It is worth noting that waves 2 and 3 have

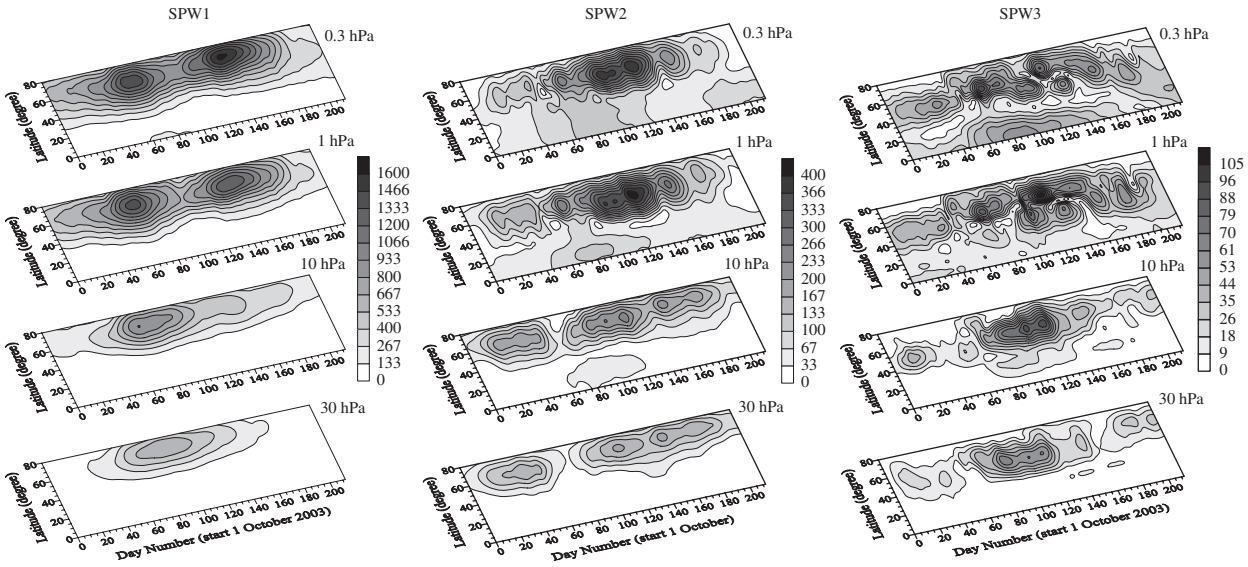

Fig. 9. Latitude–time cross sections of the amplitudes of SPW1 (left column), SPW2 (middle column) and SPW3 (right column) at four pressure levels: 30, 10, 1 and 0.3 hPa.

transient amplifications around days ~60–70 particularly strong in the upper stratosphere. Recently, Ruzmaikin et al. (2006) have examined the wavenumber dependence of the interaction between the planetary waves and zonal mean flow. The authors found that the interaction is stronger for the waves with larger wavenumber. In this way, the transient amplifications of SPW2 and SPW3 around days 60–70 could contribute additionally to the deceleration and reversal of the mean zonal wind in the high-latitude stratosphere–mesosphere system.

We note also that the amplitudes of the SPW1 and SPW2 reach their maxima at the uppermost pressure level (0.3 hPa) used for our analysis. This means that the vertical size of the SPWs forcing this major SSW is quite large and certainly covers the stratosphere and a large part of the mesosphere. This result could partly explain why the stratospheric warming spreads over into the lower mesospheric levels, as seen in Fig. 8.

6. Discussion and summary

The main focus of this paper is to study the stratosphere–mesosphere response to the major SSW in the winter of 2003/2004. The UKMO data set was used to examine the features of the large-scale thermodynamic anomalies present in the winter of 2003/2004 stratosphere of the NH. The vertical and latitudinal structure of the zonal mean temperature and zonal mean zonal wind anomalies were studied in detail. Special attention was paid to the features of the genuine anomalies associated with the SSW obtained by removing the UKMO climatology. It was found that there was no big change when the UKMO climatology was removed, but the effects were clearer. In general, the main features can be summarized as follows: (i) the zonal mean temperature and zonal mean zonal wind anomalies occur first in the upper stratosphere and penetrate down with some delay to the lower heights; the delay is particularly noticeable below 40–45 km height; (ii) the warmings at high latitudes are associated with coolings at low–middle and tropical latitudes; this compensating effect is particularly strong and interesting at 1 hPa (~48 km height) where the negative temperature pulses strengthen toward the equator; (iii) the negative wind anomalies at high latitudes are linked with the positive anomalies at low–middle and tropical latitudes and this effect is particularly strong in the upper stratosphere; furthermore, at 0.3 hPa there is a connection between the negative wind anomalies at high latitudes and alternating regions of positive anomalies in low–middle and tropical latitudes and again a negative anomaly in the equatorial latitudes. The above-mentioned effects demonstrate the strong vertical and latitudinal coupling of the thermodynamic processes in the stratosphere during the major stratwarm in the winter of 2003/2004.

The mesosphere response to the major SSW in the winter of 2003/2004 was studied by using eight radars located between 52° and 69°N (Table 1). Three of the radars are SKiYMET radars and can produce temperature around 90 km height as well as neutral winds between 81–82 and 97–98 km. It was found that, in general, the stratospheric warming was associated with upper mesospheric cooling. The negative MLT responses were clearly outlined only to the first and third temperature pulses observed in the upper stratosphere and lower mesosphere (0.3 hPa pressure level). An attempt was made to quantify this relationship. The cross correlation between the mean MLT temperature (~90 km) and the three zonal mean temperatures at 10, 1 and 0.3 hPa was calculated. The only statistically significant relationship at the 95% confidence level was that with the temperature at 0.3 hPa pressure level. The found that a negative correlation coefficient ($R = -0.39$) indicated that, in general, the lower mesosphere perturbations were out of phase with those present in the upper mesosphere levels during December/January. This result is similar to that discussed by Cho et al. (2004) based on the airglow temperature measurements and UKMO temperature data. These observational results reveal that the vertical depth of some major "stratospheric" warmings spread to the lower mesosphere levels (0.3 hPa), while the "mesospheric" cooling extends to the upper mesosphere. A possible explanation of this effect might be found in the large vertical size of the SPW1 which covers the stratosphere and a large part of the mesosphere. This result is consistent with the TIME-GCM prediction described by Liu and Roble (2002).

It was also found that the major SSW in the winter of 2003/2004 expanded to the middle latitudes, ~50°N (upper plot of Fig. 3 and middle plot of Fig. 8). We mentioned before that the stratospheric dynamics during this winter was strongly dominated by the presence of zonally symmetric waves studied in detail for the zonal wind by Pancheva et al. (2007). These waves were observed

in the temperature field as well. Similarly to the zonal wind, the waves in the temperature indicated the presence of two latitudinal branches of amplifications. The high-latitude branch was located northward of 50°N while the tropical one was centred on 20–30°N. These waves played a role in incorporating the middle latitude to the polar thermodynamic processes.

Concerning the MLT zonal wind response to the major SSW, it was found that the deceleration and reversals of the eastward winds are closely linked to the deceleration and reversal of the zonal mean zonal winds in the upper stratosphere. The mesosphere/upper stratosphere reversal of the zonal wind preceded the onset of the SSW at 10 hPa by almost 2 weeks. Dowdy et al. (2004), studying the large-scale dynamics of the MLT region during the SH major SSW in 2002, also found that the MLT zonal winds showed a reversal earlier than the 10 hPa stratospheric reversal associated with the SSW and the time difference was about 1 week. The observed time difference between the SH and NH major SSW response could be related to the strength of the polar vortex and the conditions for interaction between the planetary waves and zonal mean flow. It is known that the polar vortex in the SH is much stronger than that in the NH.

We also investigated how the MLT mean zonal wind reversal depends on the altitude (only ~80 and ~90 km altitude levels were studied) and latitude using wind data from eight radars, as four of them are situated at high latitudes (63–69°N) and the other four radars at middle latitudes (52–55°N). It was found that the mean zonal wind reversal at ~90 km height not only preceded that at ~80 km, but also reached higher westward velocity. The latitudinal dependence was considered only for ~90 km height and the result indicated that the reversal of the mean zonal wind at middle latitude slightly preceded that at high latitudes but it reached the highest westward velocity. The altitude and latitude dependence of the mesosphere eastward wind reversal reflects the basic features of the winter mesospheric jet: it amplifies with increasing the latitude and with decreasing the altitude.

It was found that the strongest negative perturbation of the MLT mean zonal wind causing significant deceleration of the winter mesosphere jet was observed near days 65–70. This wind anomaly almost coincides with the beginning of the eastward wind's deceleration in the stratosphere. The reason for this large-scale change of the stratosphere–mesosphere dynamics was the amplification of the SPW1 (left column of Fig. 9), which contributed to the bulk of westward forcing before the SSW and in this way defines the beginning of deceleration of the eastward winter mean flow. The transient amplifications of the SPW2 and SPW3 around days 60–70 contributed additionally to the deceleration and reversal of the mean zonal wind in the stratosphere–mesosphere system.

In conclusion, we note that investigating in detail the large-scale temperature and zonal wind anomalies related to the major SSW in the winter of 2003/2004 we made an attempt to demonstrate from an observational point of view the strong vertical and latitudinal coupling observed in the stratosphere–mesosphere system. The temperature relationship (based on the UKMO and meteor radar data) between the stratosphere and mesosphere during this event revealed that the vertical depth of the "stratospheric" warming spreads to lower mesosphere levels, while the "mesospheric" cooling extends to the upper mesosphere. The beginning of the eastward wind deceleration in the stratosphere–mesosphere system coincided with the maximum amplification of the SPW1 accompanied by short-lived bursts of waves 2 and 3.

Acknowledgements

We are grateful to the UKMO and the BADC for the access to the data on http://www.badc.rl.ac.uk/data/assim. We thank the anonymous reviewers for their comments on the original manuscript.

References

Cevolani, G., 1989. Long period waves in the middle atmosphere: response of mesospheric and thermospheric winds to recent minor stratospheric warmings at mid-latitudes. Annales Geophysicae 7, 451–458.

Cho, Y.-M., Shepherd, G.G., Won, Y.-I., Sargoytchev, S., Brown, S., Solheim, B., 2004. MLT cooling during stratospheric warming events. Geophysical Research Letters 31, L10104.

Coy, L., Siskind, D.E., Eckermann, S.D., McCormack, J.P., Allen, D.R., Hogan, T.F., 2005. Modeling the August 2002 minor warming event. Geophysical Research Letters 32, L07808, doi:10.1029/2005GL022400.

Dowdy, A.J., Vincent, R.A., Murphy, D.J., Tsutsumi, M., Riggin, D.M., Jarvis, M.J., 2004. The large-scale dynamics of the mesosphere–lower thermosphere during the Southern Hemisphere stratospheric warming of 2002. Geophysical Research Letters 31, L14102, doi:10.1029/2004GL020282.

Fedulina, I.N., Pogoreltsev, A.I., Vaughan, G., 2004. Seasonal, interannual and short-term variability of planetary waves in UKMO assimilated fields. Quarterly Journal of the Royal Meteorological Society 130, 2445–2458.

Gregory, J.B., Manson, A.H., 1975. Winds and wave motions to 110 km at mid-latitudes: III. Response of the mesospheric and thermospheric winds to major stratospheric warmings. Journal of the Atmospheric Sciences 32, 1676–1681.

Hartman, D.L., 1983. Middle atmospheric dynamics. Review of Geophysics and Space Physics 21, 283–290.

Hocking, W.K., 1999. Temperatures using radar-meteor decay times. Geophysical Research Letters 26 (21), 3297–3300.

Hocking, W.K., Fuller, B., Vandepeer, B., 2001. Real-time determination of meteor-related parameters utilizing modern digital technology. Journal of Atmospheric and Solar-Terrestrial Physics 63, 155–169.

Hocking, W.K., Singer, W., Bremer, J., Mitchell, N.J., Batista, P., Clemesha, B., Donner, M., 2004. Meteor radar temperatures at multiple sites derived with SkiYMET radars and compared to OH, rocket and lidar measurements. Journal of Atmospheric and Solar-Terrestrial Physics 66, 585–593.

Hoffmann, P., Singer, W., Keuer, D., 2002. Variability of the mesospheric wind field at middle and Arctic latitudes in winter and its relation to stratospheric circulation disturbances. Journal of Atmospheric and Solar-Terrestrial Physics 64, 1229–1240.

Jacobi, C., Kürschner, D., Muller, H.G., Pancheva, D., Mitchell, N.J., Naujokat, B., 2003. Response of the mesopause region dynamics to the February 2001 stratospheric warming. Journal of Atmospheric and Solar-Terrestrial Physics 65, 843–855.

Labitzke, K., 1965. On the mutual relation between stratosphere and troposphere during periods of stratospheric warmings in winter. Journal of Applied Meteorology 4, 91–99.

Labitzke, K., 1972. Temperature changes in the mesosphere and stratosphere connected with circulation changes in winter. Journal of the Atmospheric Sciences 29, 756–766.

Labitzke, K., Naujokat, B., 2000. The lower arctic stratosphere mid-winter warmings since 1952. SPARC Newsletters 15, 11–14.

Liu, H.-L., Roble, R.G., 2002. A study of a self-generated stratospheric sudden warming and its mesospheric–lower thermospheric impacts using the coupled TIME-GCM/CCM3. Journal of Geophysical Research 107 (D23), 4695, doi:10.1029/2001JD001533.

Liu, H.-L., Roble, R.G., 2005. Dynamical coupling of the stratosphere and mesosphere in the 2002 Southern Hemisphere major stratospheric sudden warming. Geophysical Research Letters 32, L13804, doi:10.1029/2005GL022939.

Lordi, N.J., Kasahara, A., Kao, S.K., 1980. Numerical simulation of stratospheric sudden warming with a primitive equation spectral model. Journal of the Atmospheric Sciences 37, 2746–2767.

Lysenko, I.A., Portnyagin, Y.I., Greisiger, K.M., Sprenger, K., 1975. Some peculiarities of the atmospheric circulation at the altitude of 90–100 km over Europe in winter 1972–73. Zeitrischrift für Meteorology 25, 213–217.

Manney, G.L., Krüger, K., Sabutis, J.L., Sena, S.A., Pawson, S., 2005. The remarkable 2003–2004 winter and other recent warm winters in the Arctic stratosphere since the late 1990s. Journal of Geophysical Research 110, D04107, doi:10.1029/2004JD005367.

Manson, A.H., Meek, C.E., 1991. Climatologies of mean winds and tides observed by medium frequency radars at Tromsø (70°N) and Saskatoon (52°N) during 1987–1989. Canadian Journal of Physics 69, 966–975.

Manson, A.H., Gregory, G.B., Stephenson, D.G., 1973. Winds and wave motions (70–100 km) as measured by a partial reflection radiowave system. Journal of Atmospheric and Terrestrial Physics 35, 2055–2067.

Matsuno, T., 1971. A dynamical model of the stratospheric sudden warming. Journal of the Atmospheric Sciences 28, 1479–1494.

Mechoso, C.R., Yamazaki, K., Kitoh, A., Arakawa, A., 1985. Numerical forecasts of stratospheric warming events during the winter of 1979. Monthly Weather Review 113, 1015–1029.

Mitchell, N.J., Pancheva, D., Middleton, H.R., Hagan, M.E., 2002. Mean winds and tides in the Arctic mesosphere and lower thermosphere. Journal of Geophysical Research 107 (A1).

Murayama, Y., Igarashi, K., Rice, D., Watkins, B., Collins, R., Mizutani, K., Saito, Y., Kainuma, S., 2000. Medium frequency radars in Japan and Alaska for upper atmosphere observations. IEICE Transactions on Communication E83-B, 1996–2003.

Myrabø, H.K., Deehr, C.S., Lybekk, B., 1984. Polar cap OH airglow rotational temperatures at the mesopause during a stratospheric warming event. Planetary and Space Science 32, 853–856.

Pancheva, D., Mukhtarov, P., Andonov, B., 2007. Zonally symmetric oscillations in the Northern hemisphere stratosphere during the winter of 2003/2004. Geophysical Research Letters 34, L04807, doi:10.1029/2006GL028666.

Perlwitz, J., Graf, H.R., 2001. Troposphere–stratosphere dynamic coupling under strong and weak polar vortex conditions. Geophysical Research Letters 28, 271–274.

Quiroz, R.S., 1971. The determination of the amplitude and altitude of stratospheric warmings from satellite-measured radiance changes. Journal of Applied Meteorology 10, 555–574.

Randel, W.J., Boville, B.A., 1987. Observations of a major stratospheric warming during December 1984. Journal of Atmospheric Science 44, 2179–2186.

Ruzmaikin, A., Cadavid, A.C., Lawrence, J.K., 2006. Stratospheric wave–mean flow interaction: simple modelling. Journal of Atmospheric and Solar-Terrestrial Physics 68, 1311–1320.

Scherhag, R., 1952. Die explosionsartigen Stratosphärenerwärmungen des Spätwinters 1951/52. Berichte des Deutschen Wetterdienstes in der US-Zone 6 (38), 51–63.

Scherhag, R., 1960. Stratospheric temperature changes and the associated changes in pressure distribution. Journal of Meteorology 17, 572–585.

Schoeberl, M.R., 1978. Stratospheric warmings: observations and theory. Review of Geophysics and Space Physics 16, 521–537.

Singer, W., Hoffmann, P., Keuer, D., Schminder, R., Kürschner, D., 1992. Wind in the middle atmosphere with partial reflection measurements during winter and spring in middle Europe. Advances in Space Research 12 (10), 299–302.

Singer, W., Bremer, J., Hocking, W.K., Weiss, J., Latteck, R., Zecha, M., 2003. Temperature and wind tides around the summer mesopause at middle and arctic latitudes. Advances in Space Research 31 (9), 2055–2060.

Siskind, D.E., Coy, L., Espy, P., 2005. Observations of stratospheric warmings and mesospheric coolings by the TIMED

SABER instrument. Geophysical Research Letters 32, L09804, doi:10.1029/2005GL022399.

Swinbank, R., O'Neill, A., 1994. A stratosphere–troposphere data assimilation system. Monthly Weather Review 122, 686–702.

Swinbank, R., Ortland, D.A., 2003. Compilation of the wind data for the upper atmosphere research satellite (UARS) reference atmosphere project. Journal of Geophysical Research 108 (D19), 4615, doi:10.1029/2002JD003135.

Walterscheid, R.L., Sivjee, G.G., Roble, R.G., 2000. Mesospheric and lower thermospheric manifestations of a stratospheric warming event over Eureka, Canada (80°N). Geophysical Research Letters 27 (18), 2897–2900.

Whiteway, J.A., Carswell, A.I., 1994. Rayleigh lidar observations of thermal structure and gravity wave activity in the high arctic during a stratospheric warming. Journal of the Atmospheric Sciences 51, 3122–3136.